A24

Rupture Processes of the Foreshocks and the Mainshock and their Correlation with the Seismicity during the Ridgecrest Earthquake Sequence (English Presentation)

○ Yijun Zhang

The 2019 Ridgecrest, California earthquake sequence included an Mw 6.4 foreshock on July 4, followed by an Mw 7.1 mainshock about 32 hours later. We determined the rupture patterns of the foreshock and mianshock by applying the automatic iterative deconvolution and stacking (IDS) method to strong motion records. The foreshock was characterized by a unilateral rupture toward the southwest, and the shallow portion had a relatively large slip with the maximum value of ~1.4 m. The mainshock presents an asymmetrical bilateral rupture with an average rupture velocity of 2.0 km/s. More than 80% of the seismic moment was released on the northwest segment of the fault, producing a maximum slip of ~5.2 m. With the two inferred slip models, we calculated the Coulomb failure stress change (ΔCFS) to analyze the spatial-temporal correlation of the seismicity activity in this sequence. The result shows that the epicenter of the Mw 7.1 mainshock was brought 0.4 bars closer to failure by the Mw 6.4 foreshock, and the stress-increased zone has a good spatial consistence with the coseismic slip distribution of the mainshock and the aftershock distribution of the foreshock. Besides, the positive ΔCFS induced by the mainshock also enhanced its aftershock activity, especially at depths of 4-10 km where the major rupture occurred, inferring that the mainshock-induced ΔCFS may be responsible for the occurrence of aftershocks. In addition, we test the effects of different cut-off frequencies and crust velocity structures on the inversion results. The result reveals that the main source rupture characteristics are almost independent of these factors, implying a high reliability of automation inversion of strong motion data. Overall, this work indicates that automatic inversion of strong motion data can provide reliable and rapid rupture model, which is essential for earthquake emergency responses and tsunami early warnings.

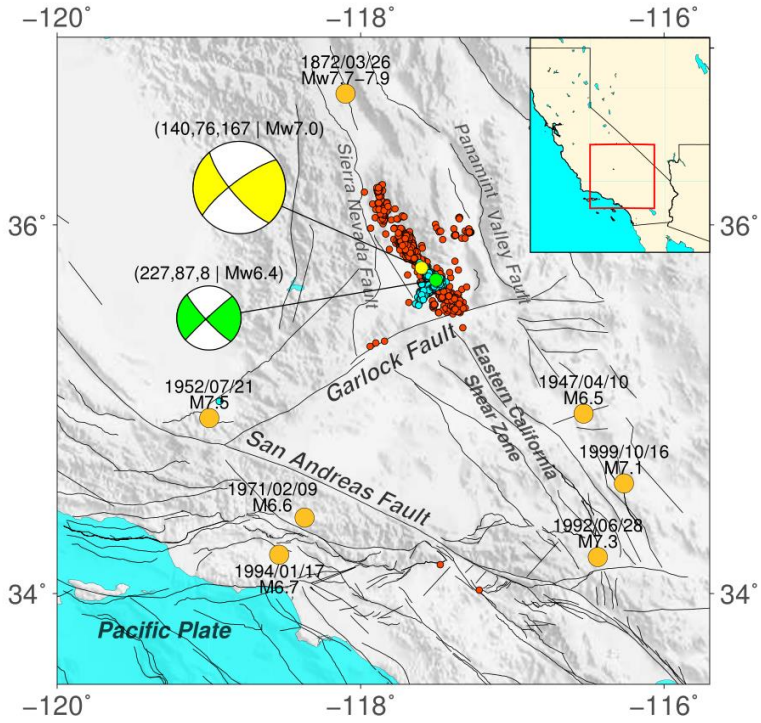
−120°
−118°
−116°
36°
34°
1872/03/26
Mw7.7–7.9
(140,76,167 | Mw7.0)
(227,87,8 | Mw6.4)
Sierra Nevada Fault
Panamint Valley Fault
Garlock Fault
Eastern California
Shear Zone
San Andreas Fault
1952/07/21
M7.5
1947/04/10
M6.5
1999/10/16
M7.1
1971/02/09
M6.6
1992/06/28
M7.3
1994/01/17
M6.7
Pacific Plate

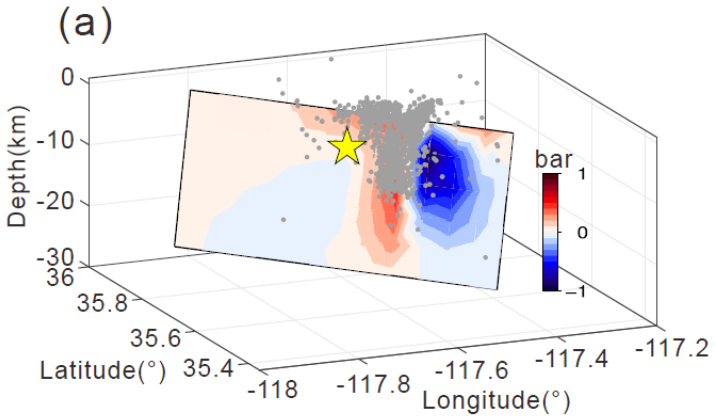
(a)
Depth(km)
0
-10
-20
-30
bar
1
0
−1
36
35.8
35.6
35.4
Latitude(°)
-118
-117.8
-117.6
-117.4
-117.2
Longitude(°)

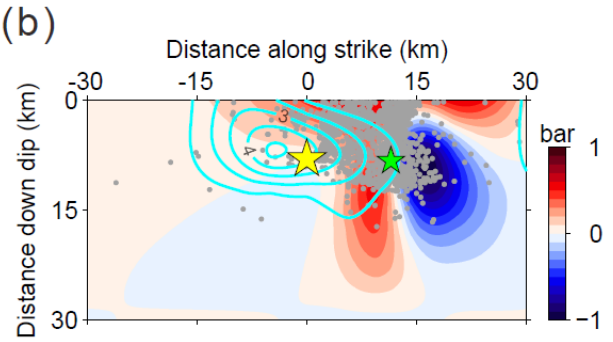
(b)
Distance along strike (km)
-30
-15
0
15
30
Distance down dip (km)
0
15
30
3
4
bar
1
0
−1